J. Fluid Mech. (1988), *vol.* 195, *pp.* 239–256
Printed in Great Britain

Onset and development of turbulence in two-dimensional periodic shear flows

By ROLAND GRAPPIN†, JACQUES LEORAT† AND PASQUALE LONDRILLO‡

†Observatoire de Meudon, CNRS UA173, F-92190 Meudon, France

‡Osservatorio di Astronomico, Universita di Bologna, Italy

(Received 13 October 1987)

We investigate numerically the time evolution of a two-dimensional flow submitted to a spatially periodic shear force. Initially, the flow is at equilibrium, the forcing balancing viscous stresses. At Reynolds numbers slightly above critical, a large-scale, linear instability drives the fluid towards a stable laminar state. At larger Reynolds number turbulence finally develops after several transient states. These transient states are described by measuring the divergence rate of linearized trajectories from the turbulent flow. This rate gives asymptotically a measure of the first Lyapunov exponent of the flow. We find that the first Lyapunov exponent scales as the characteristic frequency of the flow at large scale. We show here data on incompressible, isothermal and perfect gas (subsonic) two-dimensional flows with unit Prandtl number, and Reynolds number around 30.

1. Introduction

How does turbulence grow and develop in a fluid? Studies of bifurcations in parameter space are interesting and useful to map the possible states of a fluid, but they are generally restricted to systems with few degrees of freedom (including fluids close to a laminar state), and secondly they often ignore the path taken by the fluid to reach its final turbulent state. Phenomenology of fully developed turbulence, or closure approximations are also unable to describe the details of the transition.

We are interested here in following numerically the temporal evolution of a viscous fluid initially in an (unstable) equilibrium laminar state, with an initial Reynolds number large enough so that the fluid is expected to show a turbulent or 'chaotic' behaviour after some time. We will consider a two-dimensional flow with periodic boundary conditions in the two directions, submitted to a shearing force, periodic in space, stationary in time. The basic flow is harmonic, parallel to the $0x$-axis ($u_x = A\cos(k^f y), u_y = 0$), and forcing balances viscous stresses

$$(f_x = -\mu(k^f)^2 A\cos(k^f y), f_y = 0,$$

where μ is the viscosity). This is the so-called Kolmogorov flow (Kolmogorov 1960; Obukhov 1983).

Considering spatially two-dimensional (incompressible) periodic flows, different viewpoints may be adopted. The statistical approach was started by Kraichnan (1967), who demonstrated the possibility of an enstrophy cascade towards small scales, occurring simultaneously with an inverse energy cascade. On the other hand, a deterministic approach may be taken: the Kolmogorov flow has thus been shown

(*a*)

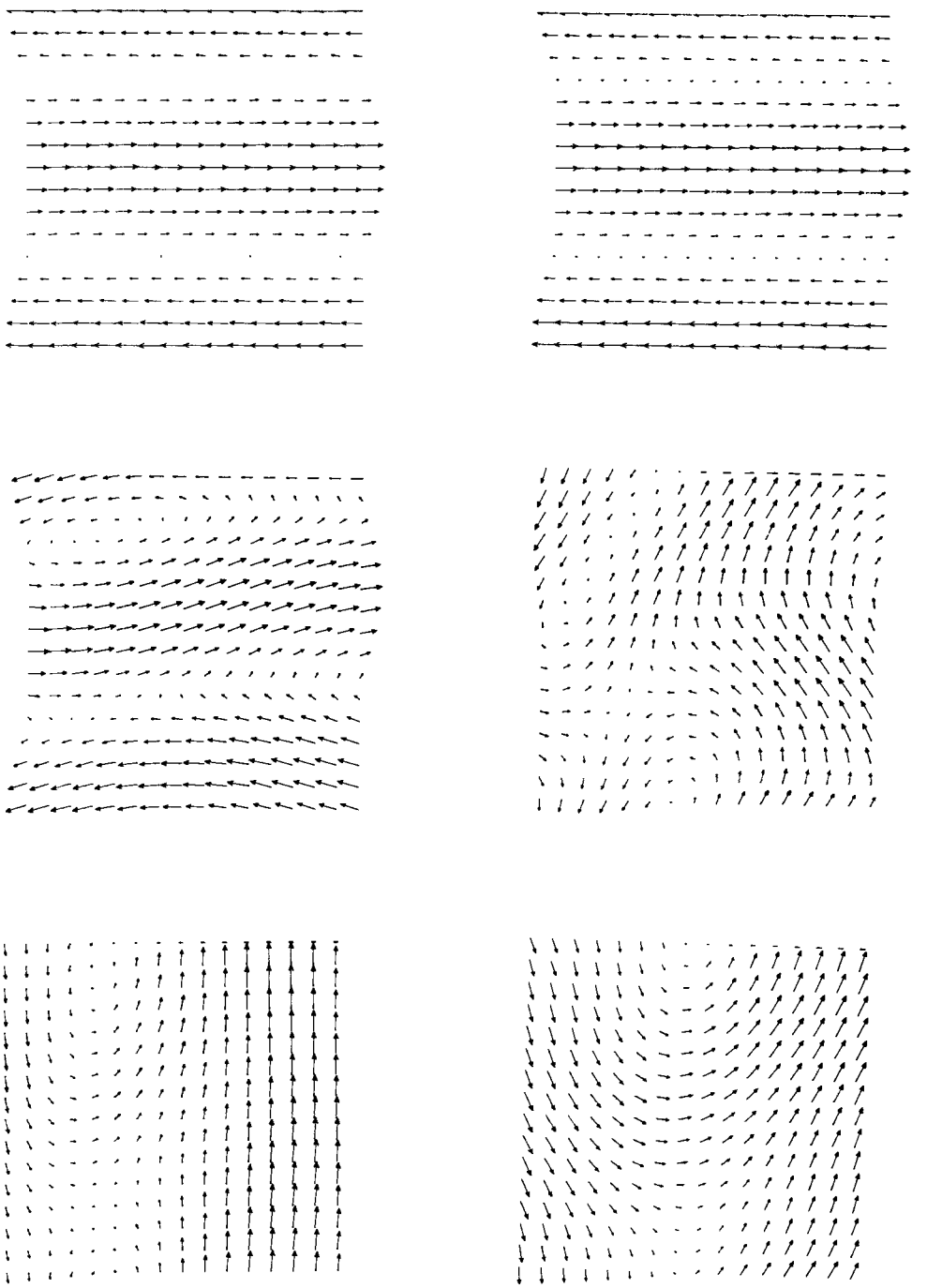

Fig. 1 (*a*). For caption see facing page.

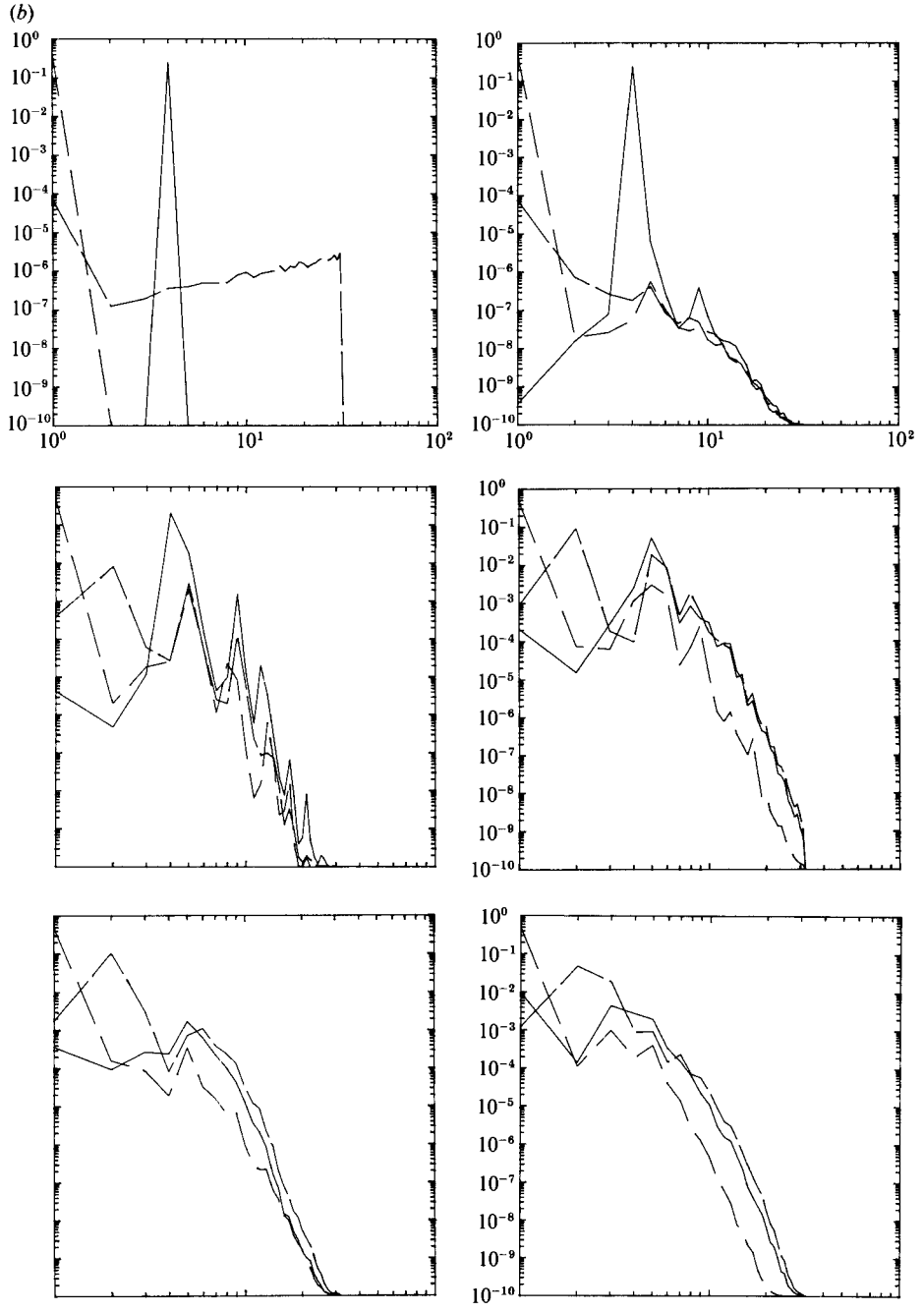

FIGURE 1. Isothermal flow: development of large-scale turbulence (run CW: initial Reynolds number $R^0 = 30$ see table 1). Successive times shown are $T = 0, 2, 8, 10, 14, 20$ s (left to right, top to bottom). (*a*) Velocity field: a quarter of the periodic squared box is shown; note that flow is almost vertical, i.e. perpendicular to the forcing direction at time $T = 14$. (*b*) Spectra: ——, x-component of impulsion); — —, y-component, and — — —, density.

to be linearly unstable to large-scale perturbation (Meshalkin & Sinai 1961; Green 1974); moreover, an asymptotic linear two-time analysis predicts a cascade of such instabilities towards larger and larger scales (Sivashinsky & Yakhot 1985).

Evidence of reverse energy transfer has been provided by experimental investigations (Couder 1984; Sommeria 1986), closure-model calculations (Pouquet *et al.* 1975), and direct numerical simulations of the two-dimensional Navier–Stokes equations (Lilly 1969; Frisch & Sulem 1984). She (1987) has studied the successive bifurcations of the Kolmogorov flow at small Reynolds numbers. Lafon (1985) has studied the case of isotropic forcing at intermediate scales.

We want here to study the fully turbulent Kolmogorov flow, by forcing at intermediary scales, so that energy can flow towards smaller as well as larger scales. We are interested by following the development of turbulence, starting from the early unstable phase, until a statistically stationary chaotic phase develops. This will be done both for incompressible and compressible (isothermal and perfect gas) flows at moderate Mach numbers (below unity).

Figure 1 gives a visual impression of the evolution of the velocity field (figure 1*a*) and spectra (figure 1*b*) so obtained, for an isothermal fluid, at Reynolds number 35, and initial Mach number 0.7, at some characteristic times of the fluid. The large-scale instability is clearly apparent.

In order to measure the temporal instability or chaos, we shall, in parallel with the Navier–Stokes equations, integrate the equations of the linearized flow (i.e. linearized around the evolving nonlinear solution). The norm of the linearized solution allows asymptotically to measure the (larger) instability rate of the attractor of the flow (or first Lyapunov exponent), following the method popularized by Benettin, Galgani & Strelcyn (1976). Lafon (1985) has applied this method to the numerical solutions of Navier–Stokes equations, for Reynolds numbers slightly above critical, with isotropic forcing. The main difference between his work and ours is that, while he looked for global measures and bifurcations, we shall try to identify successive phases in the time evolution of the flow well above threshold. Note that the isotropic forcing precludes identification of clear-cut successive large-scale instabilities; on the contrary, we will be able in this work to relate the variation of the instability rates with variations in the characteristic frequency of the fluid in the course of time.

Most calculations have been done with 64×64 points, using a Cray1S or XMP. The ratio of the largest available scale over the smallest is thus 32. The forcing scale has been mostly $\frac{1}{4}$ of the largest scale. Such a choice of parameters allows maximum (initial) Reynolds numbers which are about 30. Note that forcing at smaller wavenumbers would certainly provide a larger range to observe large-scale instabilities, but would require larger resolutions, and lead to very long times before chaos is established, as will be seen below.

2. Linear instability and first Lyapunov exponent

The two-dimensional Navier–Stokes incompressible equations read in terms of the stream function ψ (the velocity being $\boldsymbol{u} = (\partial\psi/\partial y, -\partial\psi/\partial x)$):

$$\partial\psi/\partial t = u^j(\partial\psi/\partial x^j) + F\cos(Ky) - \mu\,\Delta\psi, \tag{1}$$

where F is the forcing amplitude and μ is the viscosity. The maximum linear growth rate s of the instability of the Kolmogorov flow is, as calculated by Green (1974), equal to about one third of the characteristic frequency $\Omega^0 = Ku^0$, u^0 being the amplitude of the unperturbed flow, and K its wavenumber. Let us recall the essence

of Green's argument. We shall do that by using a Lorenz-like truncation of the (Fourier transformed) Navier–Stokes equations (1). The minimum set of interacting modes is made of the forced (sheared) mode $\boldsymbol{K}$, a perturbed one $\boldsymbol{L}$, and of two other modes ($\boldsymbol{M} = \boldsymbol{K}+\boldsymbol{L}$ and $\boldsymbol{M}' = \boldsymbol{L}-\boldsymbol{K}$) which are obtained by addition and subtraction. If we assume for simplicity that $\boldsymbol{L}$ is perpendicular to the shear wavenumber $\boldsymbol{K}$, and some symmetries (even fields, thus real Fourier components, and $\psi_M+\psi_{M'} = 0$), we are left with the following system for the three modal amplitudes: $x = \psi_K$, $y = \psi_L, z = \psi_M$:

$$\left.\begin{aligned} \mathrm{d}x/\mathrm{d}t &= 2KLyz-\mu K^2x+\tfrac{1}{2}F, \\ \mathrm{d}y/\mathrm{d}t &= -2KLxz-\mu L^2y, \\ \mathrm{d}z/\mathrm{d}t &= -KL(K^2-L^2)/(K^2+L^2)\,xy-\mu(K^2+L^2)\,z. \end{aligned}\right\} \tag{2}$$

The Kolmogorov flow corresponds to $\boldsymbol{X} = (\frac{1}{2}F/\mu K^2, 0, 0)$: this is clearly a fixed point, which is unstable when $r^{02} > 2(K^2+L^2)^2/K^2(K^2-L^2)$, where $r^0 = 2X/\mu = F/K^2$ is the initial Reynolds number. This implies a critical Reynolds number which varies from $\sqrt{2}$ (when $L = 0$) to infinity (when $L = K$). The first eigenvalue s of system (2) linearized about the Kolmogorov flow reads, expressed in terms of the amplitude of the basic flow $u^0 = F/(\mu K)$ (see equation (4) of Green's 1974 paper):

$$s/Ku^0 = -\frac{1+2(L/K)^2}{2r^0}+\left(\frac{1}{4r^{02}}+\frac{(L/K)^2\,(K^2-L^2)}{2(K^2+L^2)}\right)^{\frac{1}{2}}. \tag{3}$$

From this formula we deduce that the maximum growth at large Reynolds number obtains for a scale about half the forcing scale ($L_{\max} \approx 0.64K$), which is $s \approx 0.3Ku^0$.

More generally, if we consider arbitrary triads, we find that, at infinite Reynolds number, a triad is unstable as soon as the forced wavenumber modulus K is in between the other two. In other words, energy transfer from the forced mode is possible as soon as there is both a larger and a smaller scale available. Thus we see that the large-scale instability actually needs the presence of a 'small' scale as well. Moreover, both the smallest and the largest scales (modes L and M) grow at the same rate s.

Now, it is easily seen that, whatever the value of the Reynolds number, the three-mode system (2) always has stable fixed points, besides the preceding one. Note that system (2) can be recast in a form identical to the Lorenz equations, except for a supplementary quadratic term, which suffices to stabilize the flow. Thus, although one particular triad may possibly be unstable by itself at the start, it needs the presence, and cooperation of a larger set of modes, to reach chaos in the long term (see also Kells & Orszag 1978).

We shall thus consider a larger subset of modes, obtained by taking isotropic truncations of Navier–Stokes equations, as usual in direct numerical simulations. A mesh of 64×64 points proves to be enough to provide long-time chaotic behaviour (it allows Reynolds numbers about 30), while still respecting the physics, i.e. allowing to dissipate efficiently the energy which cascades from the injection scales down to the smallest scales.

Linear stability of the initial flow can be studied by following the evolution of infinitesimal perturbations $\delta\psi$, i.e. linearizing equation (1). To go on when the perturbation has become comparable to the mean flow, it is necessary to integrate the full Navier–Stokes equation (1) and, in order to measure the instability of the evolving fluid, to integrate in parallel with the Navier–Stokes equations, the

equation obtained by linearizing them about the nonlinear solution. The equation for the perturbed stream function $\delta\psi$ read:

$$\partial\delta\psi/\partial t = u^j(\partial\delta\psi/\partial x^j) + \delta u^j(\partial\psi/\partial x^j) + \mu\,\Delta\delta\psi. \tag{4}$$

More precisely, we will study the stability of the successive configurations of the flow by following the time evolution of the L_2 norm of the solutions of the linearized equations (4), or 'error' $\epsilon = (\int(\delta\psi)^2\,\mathrm{d}x\,\mathrm{d}y)^{\frac{1}{2}}$. Note that this definition of the error is easily generalized to compressible flows, in which the stream function is replaced by a vector field built from the velocity, density and eventually (in the perfect gas case) temperature fields.

The instantaneous error growth rate $\lambda(t) = \mathrm{d}/\mathrm{d}t\{\log(\epsilon(t))\}$ provides a measure of the local instability rate, and also of the local divergence rate of two independent nearby trajectories in phase space. The first Lyapunov exponent is the limit when T goes to infinity of the time average of the growth rate $\lambda(t)$:

$$\lambda_\infty = \lim_{T\to\infty}\frac{1}{T}\int_0^T \lambda(t)\,\mathrm{d}t = \lim_{T\to\infty}(1/T)\log(\epsilon).$$

Note that, in order to gain insight into the dynamical transition to turbulence, we will be interested below not only in estimating the asymptotic value λ_∞ but also in the transient behaviour of $\lambda(t)$.

We have integrated equations (1) and (4) in a periodic box $[0, 2\pi]\times[0, 2\pi]$. The velocity unit is given by the maximal initial velocity, which gives also the time unit, equal to the time necessary to cross a fraction $1/2\pi$ of the box at maximal velocity. The fields are defined on a squared $(N\times N)$ grid. We have modified and used two Fourier pseudospectral codes, written by Pouquet, Meneguzzi & Frisch (1986) (incompressible case), and Léorat, Pouquet & Poyet (1984) (compressible case). At resolution $N = 64$, 1000 timesteps take in the incompressible and isothermal case respectively 18 s and 35 s CPU on a CRAY1S. The time difference is due to the fact that one needs just one field (the stream function) in the incompressible case, while one needs three in the isothermal case, both cases asking for about the same number of fast Fourier transforms per timestep. The computation was carried on for several tens of thousands of timesteps.

3. The numerical experiments

We present results from simulations at resolution 64×64, with (except for the first run CW0, on which we shall first comment) Reynolds numbers around 30, Mach numbers below or equal to one, and forcing at wavelength $k^f = 4$ (see table 1). Runs are named with the following convention: the first letter indicates if the flow is incompressible (I), compressible isothermal (C), or verifies the perfect gas equation of state (P). The second letter concerns the nature of the perturbation added to the basic Kolmogorov flow: large scale (L), i.e. on a single mode (generally at half the forcing wavenumber k^f, which is the most unstable mode), or white noise (W). Both initial conditions offer a specific interest. An initial perturbation concentrated on the most unstable mode allows comparison with linear analysis during the early unstable phase. Subsequently, other large-scale modes may become unstable, but it may take a very long time before all modes become excited linearly, since the initial values of these modes are fixed by the numerical noise. On the other hand, starting with a white noise of order 10^{-3} on all modes will allow us to reach a turbulent state more

	Run	R^0	k^f	U^0	M^0
Isothermal	CW0	1.6	8	0.707	0.707
Incompressible	IL	24	4	0.707	
Incompressible	IW	24	4	0.707	
Isothermal	CL	35	4	0.707	0.707
Isothermal	CW	35	4	0.707	0.707
Perfect gas	PW	23	4	1	1

TABLE 1. Main parameters of simulations. R^0 is the initial Reynolds number, k^f the forcing wavenumber, U^0 the initial r.m.s. velocity, M^0 the initial r.m.s. Mach number.

quickly. The Reynolds number is defined in terms of r.m.s. (and not maximal) quantities; its initial value reads $R^0 = \langle\rho\rangle U^0/(\mu k^f)$, where $\langle\rho\rangle$ is the mean density, U^0 the r.m.s. amplitude of the initial velocity, μ the dynamical viscosity, k^f the wavelength of the shear (the minimum wavelength available is unity). Note that the critical value for the first bifurcation given in the preceding section, $r^0 = \sqrt{2}$, reads now $R^0 = 1$. $M^0 = U^0/c$ is the initial Mach number. In what follows, the runs will be commented on in the order of table 1: first the low-Reynolds-number isothermal run, then the 'turbulent' ones (incompressible, compressible isothermal, and perfect gas). We shall also use the integral and Taylor Reynolds numbers $R^i = \langle\rho\rangle U/\mu k^i$ and $R^T = \langle\rho\rangle U/\mu k^T$, where U is the r.m.s. velocity, and the wavenumbers are defined from the total energy spectra $E(k)$: $k^i = \int E(k)\,\mathrm{d}k/\{\int E(k)\,\mathrm{d}k/k\}$ and

$$k^T = \{\int k^2 E(k)\,\mathrm{d}k/\int E(k)\,\mathrm{d}k\}^{\frac{1}{2}}.$$

We first comment on the low Reynolds run CW0, corresponding to an isothermal flow with Reynolds $R^0 = 1.6$ slightly higher than the critical value 1, with a shear-wavenumber $k^f = 8$ (i.e. 8 wavelengths in the periodic box), and a Mach number 0.7. The y-component of the initial velocity is a white noise of small amplitude.

The main feature (shown on figure 2) is the energy transfer from the $0x$- to $0y$-component in the large scales (figure 2*c*): the final state of the flow has a substantial component perpendicular to the shear force. Moreover, the characteristic scales increase significantly (figure 2*b*), thus indicating that a large-scale instability is effective here, as in the incompressible Kolmogorov flow. However, the large-scale instability stops and the flow becomes steady and laminar after $T = 60$.

During the unstable phase, which lasts until $T = 50$ (about 280 nonlinear turnover times $t_{NL} = 1/(k^f U) = 0.18$), energy is transferred to a larger scale (the integral wavenumber k^i goes from $k^f = 8$ down to 4.5), and (partly) to the y-component of impulsion. This large-scale transfer is actually strongly anisotropic: the y-component of energy accumulates at $\frac{1}{4}k^f$, as in the linear analysis of the incompressible case at very small Reynolds numbers (cf. equation (3) and figure 1 of Green's paper), while the x-component remains peaked around k^f. Harmonics ($k = 16, 24$) grow immediately (see figure 2*c*), indicating that, in parallel with the linear large-scale instability, nonlinear transfer towards smaller scales is also at work.

All activity stops after about $T = 60$: r.m.s. values of the impulsion components and density fluctuation, characteristic wavenumbers remain constant, as well as the error ϵ, indicating a stable configuration. An estimate of the duration of the preceding unstable phase as shown on figure 1 is obtained by writing that the linearized perturbation reaches an amplitude comparable to that of the main initial shear. The saturation of the error curve suggests a zero Lyapunov exponent

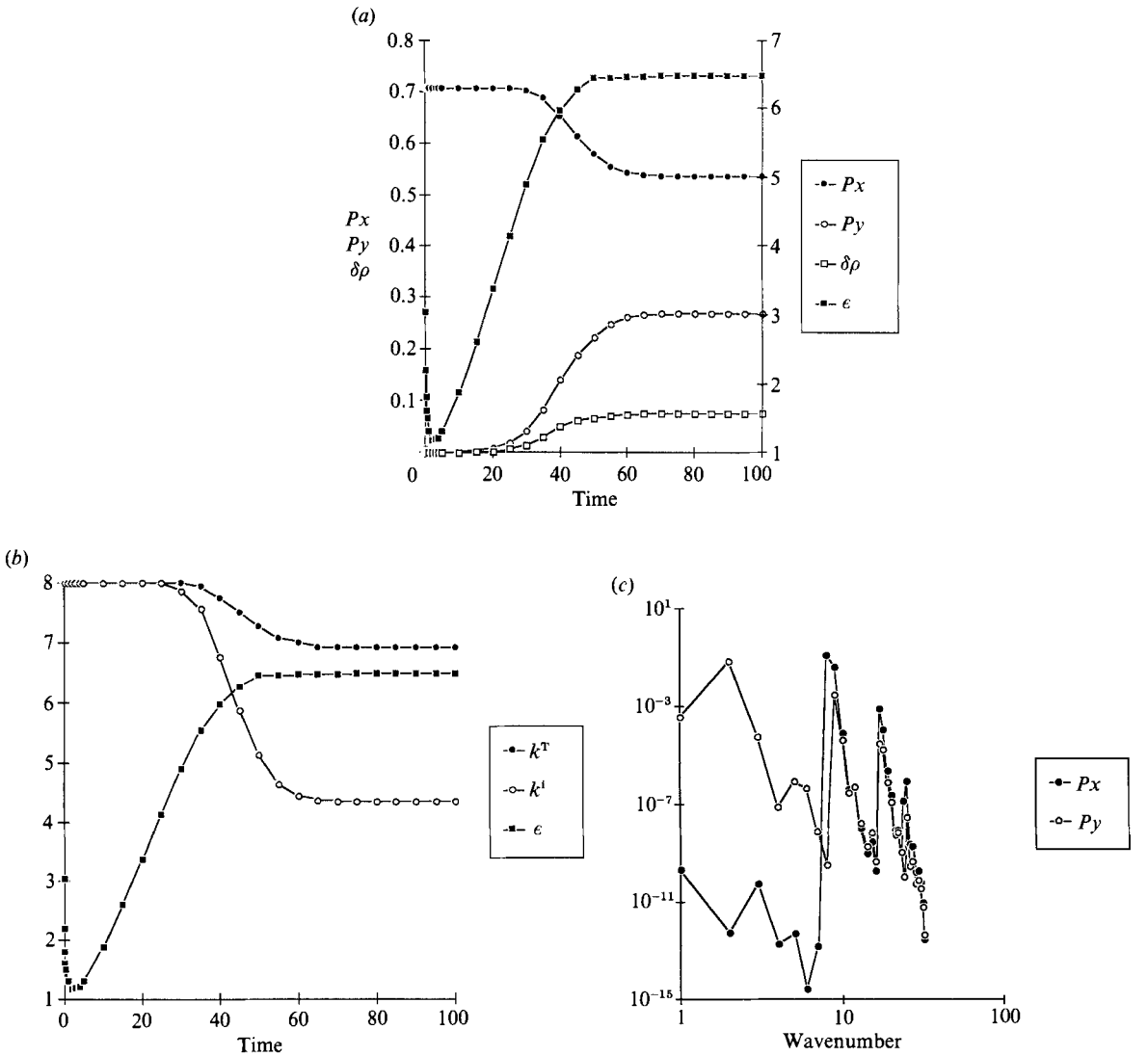

FIGURE 2. Low Reynolds number isothermal flow: development of large-scale instability followed by a laminar steady state (run CW0: $R^0 = 1.6$, see table 1). (*a*) Growth of the logarithm of the error (right-hand axis) versus r.m.s. amplitudes of nonlinear solution (x- and y-components of impulsion, and density fluctuation). (*b*) Log(error) growth versus evolution of integral and Taylor wavenumbers k^l and k^T. (*c*) Spectra of x- and y-components of impulsion (time is $T = 100$). Note that the perpendicular component dominates at wavenumbers larger than $k = 8$ at time $T = 100$ (see (*c*)). However, the maximum energy still lies at $k = 8$, which determines the total energy ratio in favour of the parallel component (see (*a*)).

$\lambda_\infty = 0$. This does not exclude strict stability. Indeed, there are always linear solutions with constant norm (constant error ϵ) hence null growth rate, corresponding to the fact that two equilibrium solutions differing by a translation parallel to the $0x$-axis remain at equilibrium: these solutions do not allow the maximal exponent to be negative. However, note that the travelling-wave solutions described by She (1987) would lead to a zero growth rate as well.

We have obtained completely analogous results for low-Reynolds-number

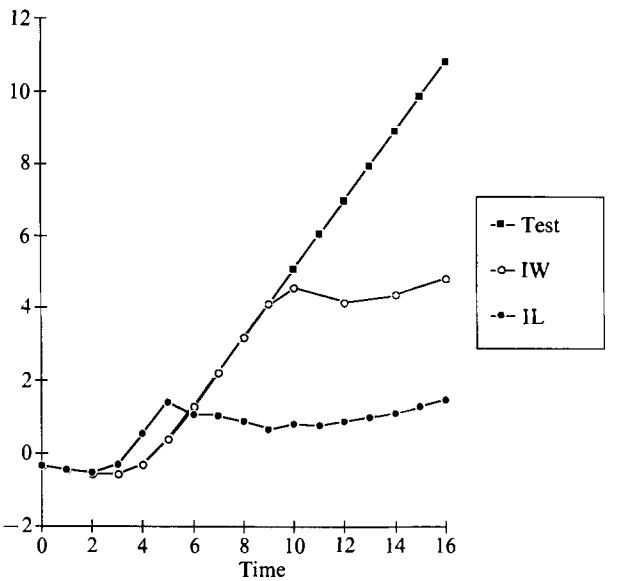

FIGURE 3. Error growth for different initial perturbations of the basic Kolmogorov flow. Curve 'test': basic flow: unperturbed steady flow. Curve IL: large-scale perturbation of the basic flow. Curve IW: white noise perturbation of the basic flow. Note that in the 'test' case, the basic flow is steady because forcing balances dissipation, and the nonlinear terms are zero. The slope of the error curve thus measures the instability rate of the basic flow, after a short period of adaptation of the error field.

incompressible Kolmogorov flows, indicating no significant differences with compressible flows at initial Mach number $M^0 = 0.71$

We now turn to the case of chaotic flows. To obtain a chaotic regime, we force at a larger scale ($k^f = 4$), so that more modes are available between the forcing scale and the smallest scales. This allows us to reach a maximum Reynolds number R^0 of about 30 at resolution 64×64. The most unstable mode of the shear flow is now the y-component at $k = 2 = \frac{1}{2}k^f$ (we are now in the large-Reynolds-number regime of Green's formula, as recalled in the preceding section).

In order to calibrate the error curve, we compare in figure 3 the instability rate of the unperturbed, stationary flow (denoted 'test' flow in the figure) and those of the perturbed flows, in the incompressible case. During a short period of time, the error first decreases. This is due to the way the initial error spectrum is prepared: all modes have comparable error amplitudes, and thus the decaying (linearly stable) modes dominate at very short times, leading to the decay of the total error ϵ. The $\log \epsilon$ curve then takes on a constant slope, which gives a measure of the linear instability rate of the initial Kolmogorov flow. This slope remains the same for all three flows, as long as the same linear instability develops. One may check that the time length of this period is found by writing that the amplitude of the perpendicular mode at $k = 2 = \frac{1}{2}k^f$ varies as $e^{\lambda t}$, where λ is the constant slope, and has reached order unity. The difference in times between runs IL and IW comes from the difference in the initial amplitude of the most unstable mode.

Notice that, contrary to the low-Reynolds-number case (run CW0), the error does not saturate: looking at longer integration times, the instability rate takes smaller, but positive values in the subsequent phases (see figure 4).

The details of subsequent evolution depends on the initial conditions. Consider

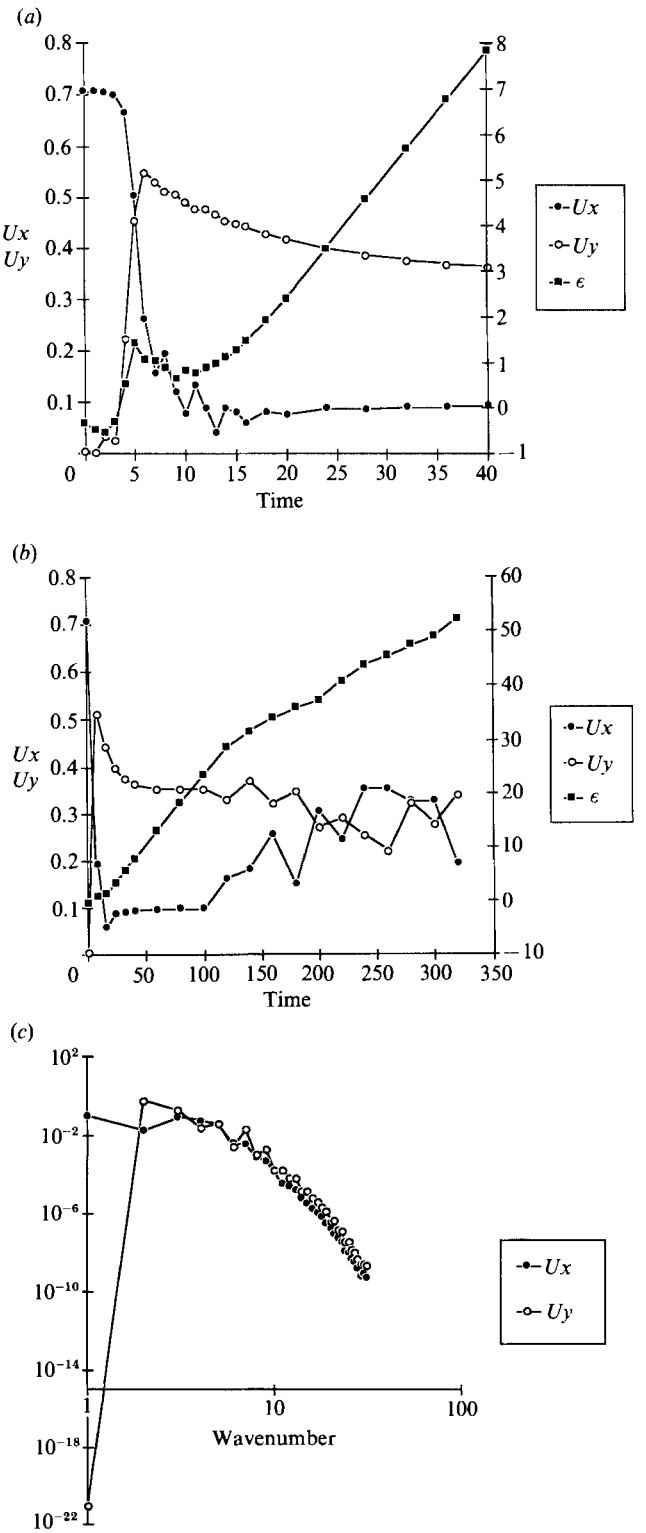

FIGURE 4. For caption see facing page.

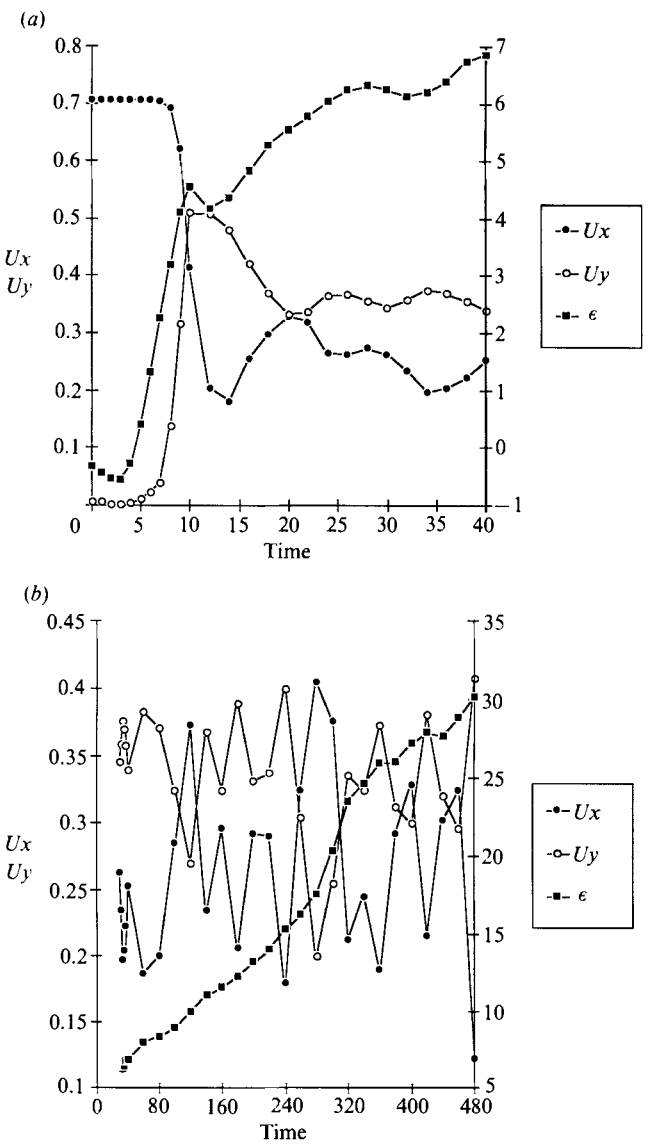

FIGURE 5. Incompressible Kolmogorov flow with white-noise perturbation: growth of the norm of the linearized solution (error) and r.m.s. amplitudes of nonlinear solution (run IW, $R^0 = 24$). (*a*) Detail of short-time evolution: growth of perturbation u_y at large scale until about $T = 10$: the y-direction is then only slightly dominant. (*b*) Later evolution: note that large-scale chaotic fluctuations start here immediately after the first instability ($T = 10$).

FIGURE 4. Incompressible Kolmogorov flow with large-scale perturbation: growth of the norm of the linearized solution (error) and r.m.s. amplitudes of nonlinear solution (run IL, $R^0 = 24$). (*a*) Detail of short-time evolution: growth of perturbation u_y at large scale until about $T = 6$. The y-component of the flow then largely dominates. (*b*) Later evolution: note the sudden onset of chaotic fluctuations at $T = 100$, and the corresponding break in the log (error) curve. (*c*) Spectra of x- and y-components of impulsion at time $T = 320$.

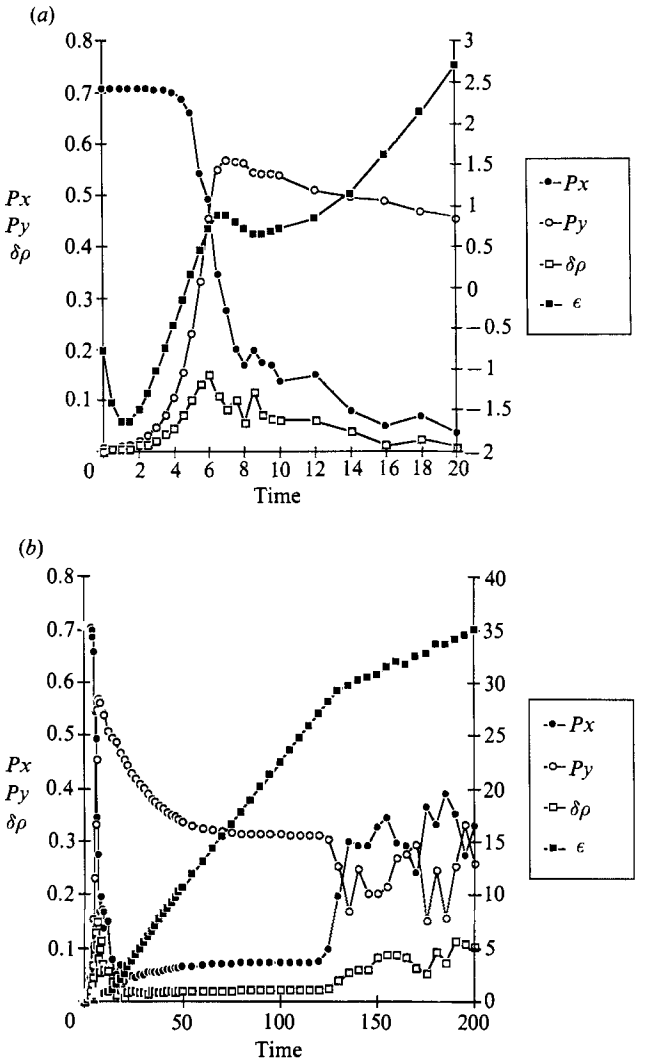

FIGURE 6. Isothermal Kolmogorov flow with large-scale perturbation: growth of the norm of the linearized solution (error) and r.m.s. amplitudes of nonlinear solution (run CL, $R^0 = 35$). (*a*) Detail of short time evolution. (*b*) Transition to turbulence: note (as in figure 4) the long transient phase with dominance of y-component, before large-scale chaos appears, and the corresponding break in the log(error) curve.

first the case of incompressible flow, with large-scale perturbation (run IL). Figures 4(*a*) and 4(*b*) show the behaviour of x and y r.m.s. components of velocity and the error. After the first instability phase, which leads to complete reversal of anisotropy, (at about $T = 4$, energy is mainly orthogonal to the forcing), there is a long period during which still larger scales develop starting from numerical noise, with a quiescent quasi-laminar flow at large scale. After about $T = 100$, these larger scales too become of order one, and a third phase begins, showing chaotic fluctuations of large-scale components. The energy spectrum shows that small scales are fully excited: compare figure 4(*c*) with the low-Reynolds-number spectrum of run CW0 (figure 2 *c*). Looking at the detailed evolution of modes shows that the y-component of impulsion at $k = 2$ grows first and saturates at about $T = 4$, then the x-component at $k = 1$ grows and

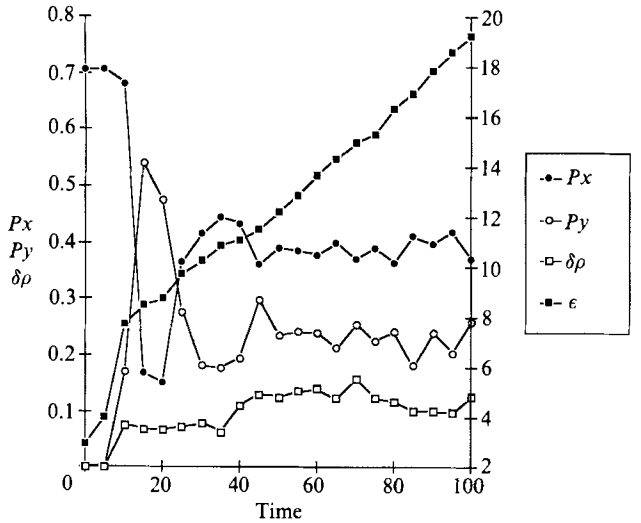

FIGURE 7. Isothermal Kolmogorov flow with white-noise perturbation: growth of the norm of the linearized solution (error) and r.m.s. amplitudes of nonlinear solution (run CW, $R^0 = 35$). Note again (as in figure 5) that chaos sets in immediately after the first instability.

saturates at about $T = 120$. The large contrast between both durations comes from the large difference in the initial amplitudes of the unstable modes: the energy of mode $(k_x = 2, k_y = 0)$ is initially about 310^{-5}, whereas for mode $(k_x = 0, k_y = 1)$, it is 10^{-30}.

A striking feature is that each of the three phases may be identified by looking at the error ($\log \epsilon$) curve: one sees three different slopes, corresponding to three different growth rates λ. Notice also that, contrary to what one would naively expect, the mean growth rate is lower for phase 2 that phase 1, and smallest for the last, chaotic phase.

If, instead of concentrating the perturbation on only one mode, we start with a white noise perturbation, we do not observe a second laminar instability phase between the first phase and the chaotic phase (run IW, figure 5). This is clearly due to the fact that all unstable modes are substantially excited at $T = 0$, and saturate at about the same time ($T = 8$ in figure 5). The average error growth rate is again lower in the final stage, although a local high slope appears around $T = 300$ (the average slope of $\log \epsilon$ is recovered after the break). This local break is coincident with a temporary predominance of the horizontal component of the flow.

We have found that isothermal flows exhibit comparable features (runs CL and CW, see figures 6 and 7). Starting from zero, the density fluctuations grow with the first instability. The phenomenology of weakly compressible turbulence predicts that the density fluctuations scale as M^2 (see Klyatskin 1966); we find here that $\delta\rho/M^2$ varies from 0.2 in the phase of large-scale instabilities to 0.5 in the chaotic phase. Again, we see in the case of large-scale initial perturbation (run CL, figure 6) three phases, with a long plateau in the second phase, during which the $0y$-component dominates, while the second quiescent phase is absent when starting with a white noise (run CW, figure 7).

In the experiments with the perfect gas equation of state, we have considered white noise initial perturbations, with an initial Mach number equal to unity (run PW). The evolution of the Mach number (figure 8*a*) shows a sudden decrease down

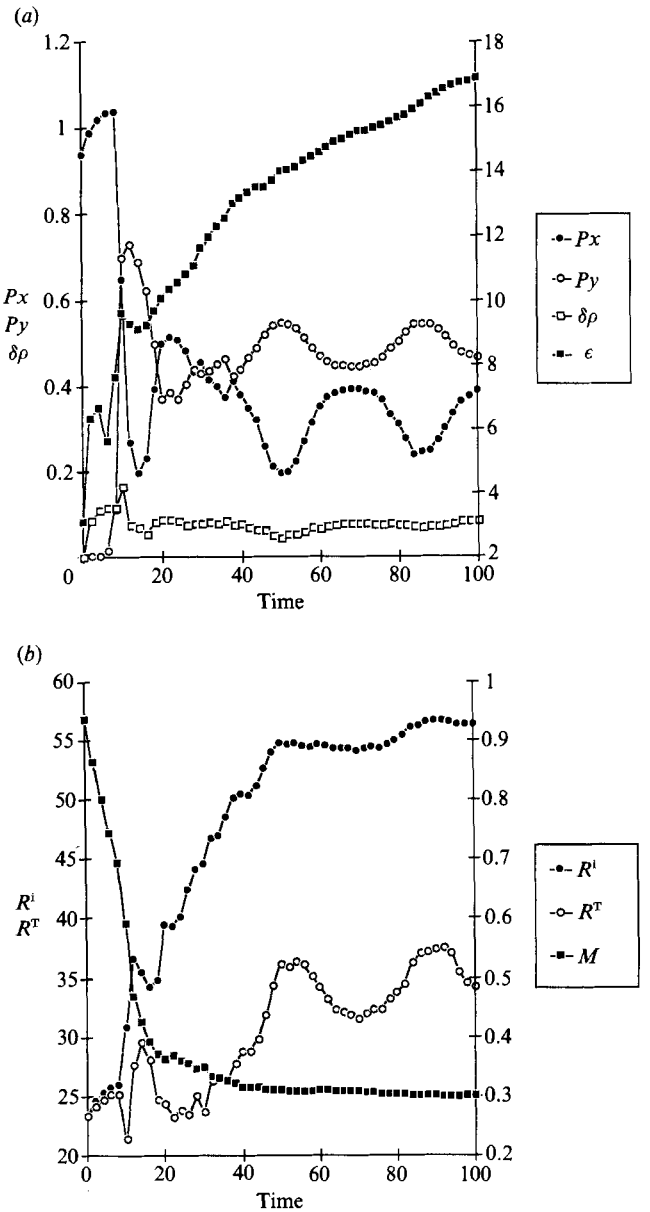

FIGURE 8. Perfect gas Kolmogorov flow with white-noise perturbation: growth of the norm of the linearized solution (error) and r.m.s. amplitudes of nonlinear solution (run PW, $R^0 = 23$). (*a*) Growth of the norm of the linearized solution and r.m.s. amplitudes of x- and y-components of impulsion and density fluctuations. (*b*) Evolution of Reynolds numbers R^i and R^T based on integral and Taylor scales, and Mach number M.

to a rather low value 0.3, followed by a slow decay: the first period corresponds to an early transfer from kinetic to internal energy, while the subsequent phase is related to a slow increase in temperature at approximately constant kinetic energy (see the quasi-constant curve of integral Reynolds number). The oscillations of the Taylor–Reynolds number after $T = 40$ correspond to the energy exchange between x- and y-components visible on figure 8(*b*), the y-component being at larger scale.

	First instability phase						Chaotic phase					
Run	T^1	T^2	λ	U	k^i	λ/Ω	T^1	T^2	λ	U	k^i	λ/Ω
IL	3	5	0.86	0.7	4	0.31	120	320	0.12	0.41	1.80	0.16
IW	3	10	0.73	0.7	4	0.26	10	480	0.05	0.45	1.11	0.11
CL	2	6	0.55	0.7	4	0.20	140	200	0.08	0.40	1.78	0.11
CW	5	10	0.75	0.7	4	0.27	10	100	0.13	0.48	1.70	0.16
PW	6	10	1.01	1.0	4	0.25	40	100	0.06	0.59	1.08	0.10

TABLE 2. Characteristic quantities of the flow in the first and last phases. k^i is the integral wavenumber. U is the average r.m.s. velocity. Ω is the characteristic frequency of the flow ($\Omega = k^i U$). In the first phase, k^i is close to the forcing wavenumber k^f, and U is close to the initial value U^0. λ is the average divergence rate of trajectories in phase space (estimated between times T^1 and T^2). Its value in the chaotic phase is an estimate of the first Lyapunov exponent of the turbulent attractor.

The r.m.s. components show several phases (see figure 8*a*): first, the x-component grows, then saturates (while the y-component grows), then both components exchange themselves in a random way, and finally they slowly oscillate. To each of the four successive phases corresponds a different average slope of the error curve. One finds that the characteristic period of the long oscillations is near to about $2/\lambda$, where λ is the instability rate evaluated on the corresponding time interval (50, 100). Remark that such long-period, large-scale fluctuations are also visible in the other (incompressible and isothermal) runs, although less regular and more chaotic (see figures 4*b*, 5*b*, 6*b*, 7).

Note that in the perfect gas experiments, we cannot reach a stationary state, since we inject kinetic energy and thus accumulate thermal energy generated by viscous stresses. Note also that, due to increase of thermal energy, the Mach number quickly drops from one to about 0.3. This value has also been found in free decay calculations (Passot & Pouquet 1987).

4. Discussion

Two different physical processes are at work in the flow studied here: at first, an exponential growth of linear unstable modes at large scales, then eventually, as the largest scales become saturated, the onset of turbulence (all modes participating nonlinearly). There is a good agreement between compressible and incompressible runs, in the range of Mach numbers considered (up to one initially, but note that the final r.m.s. values are much lower, smaller than 0.4).

An important feature of the flow in its chaotic state is the ability to develop long period (and large scale) chaotic fluctuations of velocity after a preliminary quick rise of these large scale components. This process is well illustrated by the piecewise monotonic growth of the error curve as a function of time: the slope is always lower in the last, chaotic phase. Why does the last, chaotic phase possess the slowest timescale? This could be due simply to the excitation of the largest scales having lower characteristic frequencies. In order to test this hypothesis, we have rescaled the divergence rates by dividing them by the characteristic frequency Ω, defined as the product of the integral wavenumber k^i and r.m.s. velocity U. Table 2 summarizes the data obtained in the first instability phase and the chaotic phase: we have indicated the time intervals $[T_1, T_2]$ between which the instability rates λ are

measured. Rescaling is seen to reduce much of the variation of λ: the early rescaled values gather around 0.3, while the last phase's values are about 0.1.

Note that the first relation, $\lambda = 0.3\Omega$, agrees reasonably well with that found analytically by Green (1974). Relation (3) gives, at Reynolds number 35,

$$s = 0.25Ku^0 = 0.36\Omega$$

since there is a factor $\sqrt{2}$ between r.m.s. and maximum values of the velocity (respectively U^0 and u^0).

Similar agreement can also be found in the intermediary phases of large-scale transfer (not given in the table) although the flow at that time is different from the initial Kolmogorov flow considered by Green. For instance, we find for run CL between $T = 20$ and $T = 130$, $\lambda \approx 0.23$ and $\lambda/\Omega \approx 0.32$ (see figure 6*b*).

The fact that, even after rescaling, the divergence rate still appears significantly lower in the turbulent phases may be explained in several ways. It may be due to Ω being a too rough a measure of the intrinsic frequency of the flow, or to the numerical algorithm: in the early quasi-linear phase, λ gives effectively the maximal instability rate, while in the chaotic phase, where the eigenfunctions of the system change more quickly with time, the algorithm might give a lower average.

There is good quantitative agreement, in the chaotic regime, between the timescales (inferred from visual inspection) of the large-scale fluctuations of r.m.s. components of velocities and the values of the divergence rate λ: first the quasi-linear growth of the perpendicular component occurs with a characteristic time of about 3 turn-over times; then the chaotic fluctuations have a longer timescale, around 20 turn-over times. These long timescales may be related to the absence of substantial excitation of small scales in the two-dimensional flows studied here, as opposed to three-dimensional flows.

A similar scaling of the first Lyapunov exponent with the characteristic frequency ($\lambda = 1/3\Omega$) has already been found in the framework of a model of three-dimensional turbulence (Grappin, Léorat & Pouquet 1986): in the latter work, the characteristic frequency is determined by the small scales of the flow, and is many orders of magnitude greater than the values obtained here, where the characteristic frequency is that of the large scales.

To the relative smallness of the first Lyapunov exponent of two-dimensional Kolmogorov flows corresponds the smallness of the Lyapunov dimension, which has been found to be around 10 when $k^f = 2$ and 25 when $k^f = 4$, although the system has several thousand degrees of freedom (Grappin & Léorat 1987).

In conclusion, we have found that in two-dimensional Kolmogorov flow, the chaotic timescale, as given either by large-scale r.m.s. fluctuations or by the largest Lyapunov exponent is based on the largest scales available in the simulation. We have performed higher resolution runs (128×128 points, initial Reynolds number $R^0 = 70$, average integral Reynolds number $R^i \approx 130$), which show that the scaling of the largest Lyapunov exponent on the characteristic frequency does not depend on the Reynolds number, as soon as it is above critical, say larger than 10. Comparison between the incompressible and compressible runs reported here shows that our result does not depend on the Mach number for subsonic flows either. For turbulent flows with more realistic boundaries, one may ask if the scaling law for the first Lyapunov exponent remains valid.

These considerations have some bearing on the predictability concept. The predictability of large-scale circulation in the atmosphere and oceans is affected by the growth of observational errors which contaminate larger and larger scales,

starting from the lack of determination of small scales of motion (Thompson 1957; Lorenz 1969). Although predictability issues may be posed entirely in a linear context, numerical studies usually consider an error whose initial growth is ruled by nonlinear transfer from small to large scales. The error we have considered here has two characteristics: it is a linearized quantity, and it takes all scales into account, being a (quasi-) L_2 norm of the linearized solution. A comparison between predictability results and Lyapunov timescales needs a discussion of the ratio of the nonlinear large-scale transfer of the error to the instability rate at large scales. In the case of closure approximation like EDQNM (Herring 1983; Métais & Lesieur 1986), since linear instabilities are absent from the approximation, the predictability time is given by a nonlinear (inverse) transfer time. Similar computations by direct simulations would require to integrate two nonlinear solutions of the Navier–Stokes equations, differing initially only in the small scales.

Research on the same kind of forced flows, now in progress, includes modelling both the large-scale instability and the onset of turbulence, and computation of Lyapunov exponents in three-dimensional flows.

We thank the Scientific Committee of the Conseil Scientifique du Centre de Calcul Vectoriel pour la Recherche (CCVR) and University of Bologna, Institute of Astronomy who provided the computational facilities. This work received financial support from the CNRS through the RCP 'Fluides astrophysiques en régime supersonique' and the ATP 'Dynamique des fluides géophysiques et astrophysiques'. We acknowledge several interesting discussions with Z. S. She.

A shortened version of this paper was presented at the 6th Colloquium 'Turbulent Shear Flows', held in Toulouse, France, September 1987.

REFERENCES

Benettin, L., Galgani, L. & Strelcyn, J. M. 1976 *Phys. Rev.* A **14**, 2338.

Couder, Y. 1984 Two-dimensional grid turbulence in a thin liquid film. *J. Phys. Lett.* **45**, 353–360.

Frisch, U. & Sulem, P. L. 1984 Numerical simulation of the inverse cascade in two-dimensional turbulence. *Phys. Fluids* **27**, 1921.

Grappin, R., Léorat, J. & Pouquet, A. 1986 Computation of the dimension of a model of fully developed turbulence. *J. Phys. Paris* **47**, 1127.

Grappin, R. & Léorat, J. 1987 Computation of the dimension of two-dimensional turbulence. *Phys. Rev. Lett.* **59**, 1100.

Green, J. S. A. 1974 Two-dimensional turbulence near the viscous limit. *J. Fluid Mech.* **62**, 273.

Herring, J. R. 1983 The predictability of quasi-geostrophic flows. Proc. AIP Conf. No. 106. In *Predictability of Fluid Motions* (ed. G. Holloway & B. J. West), pp. 321–332.

Kells, L. C. & Orszag, S. A. 1978 Randomness of low-order models of two-dimensional inviscid dynamics. *Phys. Fluids* **21**, 162.

Klyatskin, V. I. 1966 *Izv. Atmos. Ocean. Phys.* **2**, 474.

Kolmogorov, A. N. 1960 In Seminar Notes ed. V. I. Arnold & L. D. Meshalkin. *Uspekhi Mat. Nauk* **15**, 247.

Kraichnan, R. H. 1967 Inertial ranges in two- and three-dimensional turbulence. *Phys. Fluids* **10**, 1417–1423.

Lafon, A. 1985 Etude des attracteurs pour des écoulements bidimensionnels de fluides visqueux incompressibles. Thèse d'état, Université Paris VI.

Léorat, J., Pouquet, A. & Poyet, J. P. 1984 Numerical simulations of supersonic turbulent flows. In *Problems of Collapse and Numerical Relativity*, p. 287. Reidel.

LILLY, D. K. 1969 *Phys. Fluids Suppl.* **12**, 240.

LORENZ, E. N. 1969 The predictability of a flow which possesses many scales of motion. *Tellus* **21**, 289–307.

MESHALKIN, L. D. & SINAI, YA. G. 1961 *Z. angew. Math. Mech.* **25**, 1700.

MÉTAIS, O. & LESIEUR, M. 1986 *J. Atmos. Sci.* **43**, 857.

OBUKHOV, A. M. 1983 *Russ. Math. Surveys* **38**, 113.

PASSOT, T. & POUQUET, A. 1987 Numerical simulations of compressible homogeneous flows in the turbulent regime. *J. Fluid Mech.* **181**, 441.

POUQUET, A., LESIEUR, M., ANDRÉ, J. C. & BASDEVANT, C. 1975 *J. Fluid Mech.* **72**, 305.

POUQUET, A., MENEGUZZI, M. & FRISCH, U. 1986 *Phys. Rev.* A **33**, 4266.

SHE, Z. S. 1987 Large scale dynamics and transition to turbulence in two dimensional Kolmogorov flows. Preprint Observatoire de Nice, France.

SIVASHINSKY, G. & YAKHOT, V. 1985 Negative viscosity effect in large-scale flows. *Phys. Fluids* **28**, 1040.

SOMMERIA, J. 1986 Experimental study of the two-dimensional inverse energy cascade in a square box. *J. Fluid Mech.* **170**, 139.

THOMPSON, P. D. 1957 Uncertainty of initial state as a factor in the predictability of large-scale atmospheric flow patterns. *Tellus* **9**, 275–295.